Original Article

JHSMR Journal of Health Science and Medical Research

Development of an Antibody Targeting Variants of the SARS-CoV-2 Spike Protein

Puridech Bubphamanee, B.Sc.[1], Praopim Limsakul, Ph.D.[2], Krit Charupanit, Ph.D.[1], Thana Sutthibutpong, Ph.D.[3], Pemikar Srifa, Ph.D.[1]

[1]Department of Biomedical Sciences and Biomedical Engineering, Faculty of Medicine, Prince of Songkla University, Hat Yai, Songkhla 90110, Thailand.

[2]Division of Physical Science, Faculty of Science, Prince of Songkla University, Hat Yai, Songkhla 90110, Thailand.

[3]Theoretical and Computational Physics (TCP) Group, Department of Physics, King Mongkut's University of Technology Thonburi (KMUTT), Bangkok 10140, Thailand.

Received 31 August 2024 ● Revised 6 September 2024 ● Accepted 6 September 2024 ● Published online 14 February 2025

Abstract:

Objective: The novel coronavirus severe acute respiratory syndrome coronavirus 2 (SARS-CoV-2), which enters human cells through its spike protein binding the human receptor (ACE2), has evolving variants of concern (VOCs). This *in silico* study aimed to enhance the binding efficacy of a fragment in the SARS-CoV-2 antibody, by designing single-chain variable fragments (scFv) to block ACE2 from binding various receptor binding domain (RBD) variants.

Material and Methods: The modified scFv structures were derived from the regdanvimab (CT-P59) IgG antibody. The binding interactions between the scFv and RBD of VOC variants were characterized using molecular docking and molecular dynamic (MD) simulations. Additionally, computational mutagenesis was also performed to optimize the scFv binding efficacy against the RBD variants.

Results: The unmodified CT-P59 scFv exhibited stronger binding affinities to VOC variants as compared to those of the Fab fragment; except for the Beta and Omicron XBB.1.5 variants. The docking results of the mutated antibody revealed that the R105W mutation in the scFv exhibited the most significant improvement in binding affinity across all VOCs. Additional MD simulation showed that the R105W mutation resulted in stronger binding affinity and stability than those of the wild-type CT-P59 Fab fragment; particularly against the Delta and Omicron variants. The R105W mutation induced binding by consistently interacting with virus-conserved residues Y452, F486, and Y489 on the RBD.

This paper was from The 3rd Annual Health Research International Conference (AHR-iCON, August 29-30, 2024).
Contact: Pemikar Srifa, Ph.D.
Department of Biomedical Sciences and Biomedical Engineering, Faculty of Medicine, Prince of Songkla University, Hat Yai, Songkhla 90110, Thailand.
E-mail: pemikar.s@gmail.com

J Health Sci Med Res .....
doi: 10.31584/jhsmr.20251152
www.jhsmr.org

Conclusion: This study successfully highlights the potential of the scFv with R105W mutation, targeting conserved RBD regions. This suggests that $scFv_{R105W}$ is a promising therapeutic candidate against SARS-CoV-2. Additionally, it provides a framework for developing potent therapeutic antibodies against COVID-19 and potential future pandemics; emphasizing the importance of adaptive strategies in response to viral mutations.

Keywords: molecular docking, molecular dynamic (MD) simulation, mutagenesis, single-chain variable fragments (scFv), variants of concern (VOCs)

Introduction

The emergence of severe acute respiratory syndrome coronavirus 2 (SARS-CoV-2) in late 2019 led to the coronavirus disease 2019 (COVID-19) pandemic. The viral spike protein on the surface of SARS-CoV-2 plays a critical role in infection by binding to the human cell receptor, angiotensin-converting enzyme 2 (ACE2) via its receptor binding domain (RBD). This interaction is essential for viral entry[1,2].

Monoclonal antibodies targeting the spike protein-ACE2 interaction offer a promising treatment approach[3,4]. While the severity of the initial COVID-19 strain lessened with widespread vaccination, ongoing mutations have led to the emergence of variants of concern (VOCs) with increased transmissibility and virulence, necessitating adaptations in public health strategies[3].

Crucially, mutations in the SARS-CoV-2 RBD and receptor binding motif (RBM) can significantly reduce antibody effectiveness. This study focuses on these critical mutations in emerging VOCs, excluding Alpha and Gamma due to their limited impact. While the Alpha variant possessed a single mutation (N501Y) on the RBD, it has largely been outcompeted by more transmissible variants like Delta and Omicron. Although both Gamma and Beta share the concerning RBM mutations (E484K and N501Y), research suggests Gamma poses a lower risk of re-infection and reduced immunity[5]. The Delta variant has distinct mutations in the RBM (L452R and T478K), while the Omicron variant presents a complex picture with over 30 mutations across its spike protein. In the BA.1 subvariant, eight RBM mutations (N440K, G446S, S477N, T478K, E484A, Q498R, N501Y, and Y505H) overlap with all Omicron mutations while Q493R and G496S were found only in the BA.1. Notably, the BA.1 subvariant possesses the S477N mutation, which is absent from BA.2. Notably, the BA.4 and BA.5 subvariants share the same RBM mutations (L452R and T478K) as Delta variant, and the Omicron XBB.1.5 variant carries 12 RBM mutations, including F486P, which is believed to enhance its binding affinity to ACE2, potentially explaining its increased transmissibility[5].

To address these challenges, we propose a computational approach to design effective antibodies against VOCs. By utilizing molecular docking and molecular dynamic (MD) simulations, we identify antibodies with the ability to bind to a wide range of VOC spike protein variants. Binding energy assesses the strength of the antibody-virus interaction. This approach has the potential to yield a potent therapeutic antibody for COVID-19 and provide a valuable framework for developing treatments against future viruses with similar characteristics.

Material and Methods

The overall simulation process comprises several key steps. Initially, the structural modifications of monoclonal antibodies used in this work were done based on a SARS-CoV-2 drug called regdanvimab or CT-P59 (DrugBank

Accession Number: DB16405), which is designed for SARS-CoV-2. Then, seven RBD protein structures, including wild-type (WT) and 6 VOCs, were collected and prepared for subsequent drug-protein interaction analyses.

The simulations were conducted with multiple objectives. Molecular docking, coupled with MD simulations, was employed to characterize the binding properties between the modified antibodies (Fab and scFv; detailed below) and each structure of RBD variants. The following step was to enhance drug efficacy by mutagenesis of scFv residues.

Lastly, molecular docking calculations were performed to analyze the interactions between each mutated drug and VOCs. Details of each step are provided below. Below are the details of each step involved in this work.

The structural modification of drugs

The scFv model was constructed using SWISS-MODEL (https://swissmodel.expasy.org/, accessed on 26 October 2023). The initial model was obtained from the sequences of variable heavy chain (VH) and light chain (VL) fragments of regdanvimab or CT-P59, a SARS-CoV-2 neutralizing monoclonal antibody in its full immunoglobulin (IgG) form[4] (Figure 1a). The structure was connected by a flexible linker (GGGGSx3) which this linker imparts flexibility to the structure[6].

Selection of SARS-CoV-2 related proteins

Seven proteins representing active areas of each SARS-CoV-2 variant were taken from the Protein Data Bank (PDB, https://www.rcsb.org/). The RBDs of SARS-CoV-2 VOCs were derived from the spike protein structures available in the following PDB entries: Wild type (6M0J), Beta (7R17), Delta (7W92), Omicron BA.1 (8DM9), Omicron BA.2 (7XIW), Omicron BA.4 (7XNQ), and Omicron XBB.1.5 (8JYM).

Model preparation and Molecular docking

In this research, a software program called HADDOCK2.4 (https://wenmr.science.uu.nl/haddock2.4/, accessed on 26 October 2023) was employed to perform molecular docking calculations in the first step of predicting complex binding postures between the scFv model and the target proteins of SARS-CoV-2[7,8].

To prepare the protein structures for molecular docking calculations, any water molecules and non-protein residues were removed. Both scFv and each of the SARS-CoV-2 RBDs participated in protein-protein docking with HADDOCK. The calculated docking parameters were *COVID-19-related* ones. The active site of scFv was defined by complementarity-determining regions (CDRs) and the active site of RBD was defined based on RBM[9].

During molecular docking calculations, resulted in docking complexes were retrieved along with their binding score which reflects the strength of interactions between each protein pair. Afterward, the retrieved complex underwent further MD simulations to gain further insights into the molecular interactions between the scFv and the SARS-CoV-2 target proteins.

MD simulations and MMPBSA

MD simulations were performed to optimize the protein complex and simulate explicit solutions using the GROMACS 2024.1 software package and CHARMM36 forcefield[10,11]. The molecular mechanics/Poisson-Boltzmann solvent accessible surface area (MM-PBSA) method was utilized to analyze the binding free energy in the equilibrium state following MDs run to analyze modification mutations further. The initial complex was taken from molecular docking by HADDOCK2.4 with the lowest binding energy (most negative), selected as the starting conformation for the MD simulations.

The scFv antibody-RBD complex structures from the previous molecular docking were explicitly solvated with the TIP3P water model in a periodic water box and were neutralized by adding Na^+ and Cl^- counterions with 0.15 M

salt concentration. Each simulation was subjected to using the steepest descent algorithm for energy minimization, and system equilibration was achieved by position-restrained dynamic simulations (NVT and NPT ensembles) at 300 K for 100 ps. Subsequently, the entire system underwent an MD run at a temperature of 300 K and pressure of 1 bar for 100 ns. Relative binding energies from the MD simulations were calculated and compared to those of Fab-VOCs, which were performed in another calculation set.

Computational mutagenesis of scFv

Five residues of scFv were selected to perform single point mutation by replacing with other amino acids representing various properties: hydrophobic (isoleucine), polar (serine/threonine), positively charged (lysine/arginine), negatively charged (aspartic acid/glutamic acid), and bulky (tryptophan). Subsequently, each singly mutated antibody was subjected to dock with the RBD of VOC variants to assess alterations in their binding interfaces. The variant demonstrating the most negative docking score was chosen for detailed investigation using MD simulations.

Results

CT-P59 antibody fragment and binding energy against variants coronavirus RBD

All the modified antibodies in this study were derived from a monoclonal antibody CT-P59 in its fully immunoglobulin (IgG) form[4]. The IgG consists of two fragments of antigen-binding (Fab) separated into four regions. In each Fab, the virus-binding site consists of a light chain (VL) connected to a heavy chain (VH)[9]. This region was cut and remodeled in this work to represent only the effective binding region as a single-chain variable fragment of CT-P59, named scFv. The small scFv structure contains various CDRs representing the antigen-binding sites that can interact directly with the epitope (Figure 1b).

To investigate the binding conformation of the modified drug and the VOCs, Both Fab and scFv were used in comparative MD simulations. A single residue binding energy (ΔG_{res}) of scFv and RBD_{WT} in equilibrium was collected and compared to those of FAB. Interestingly, the Fab utilized only heavy chains featuring CDRH3 residues L104, R105, Y106, and R107 to bind with the wild-type RBD, whereas the scFv utilized both chains with residues R105 and S237 (Figure 2a). Both complexes indicate that the conserved active region R105 on the CDRH3 is a significant binding residue, exhibiting the lowest binding energy ΔG_{res} (supporting information; Supplementary Figure 1, 2).

The Fab antibody showed the most negative binding energy to RBD_{WT} and higher binding energies when interacting to the variants, indicating the weaker binding forces to the variants of the coronavirus. Overall results showed that the scFv demonstrated more negative binding energy than those of Fab, except in the complexes of Beta and Omicron XBB.1.5 variants (Figure 2b). The binding energies at residues R105 and S237 of scFv increased in other variants, showing lower interactions around these sites. These changes affected the decrease of binding energies in neighbor residues, such as L104, Y106, R107, W235, and S240 (Supplementary Figure 2 of supporting information). There was no light chain interaction found in the complexes of scFv binding to Beta and Delta variants.

Screening of scFv mutant against VOC via molecular docking.

Five amino acid residues of the scFv were selected for mutagenesis to enhance binding properties against VOCs. These residues were chosen based on their substantial impact on interactions with the virus, as indicated by their binding energies. The five residues are: D56, R99, R105, D116, and S237 (shown in Figure 3a). Other 5 amino acids that used to single replace those 5 residues are Isoleucine (I), Serine (S), Glutamic Acid (E), Lysine (K), and Tryptophan (W).

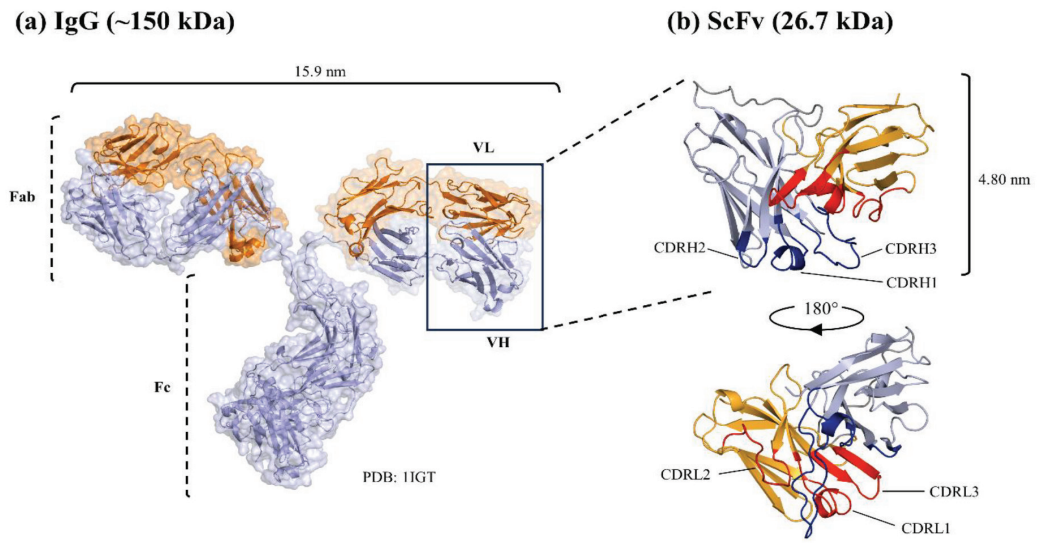

Figure 1 (a) Overview of the crystal structure of IgG. (b) The structure of the scFv is shown in a ribbon diagram. The CDRs are highlighted, with the light chain (CDRL) shown in red and the heavy chain (CDRH) demonstrated in dark blue. The heavy chain is shown in light blue and, the light chain in orange

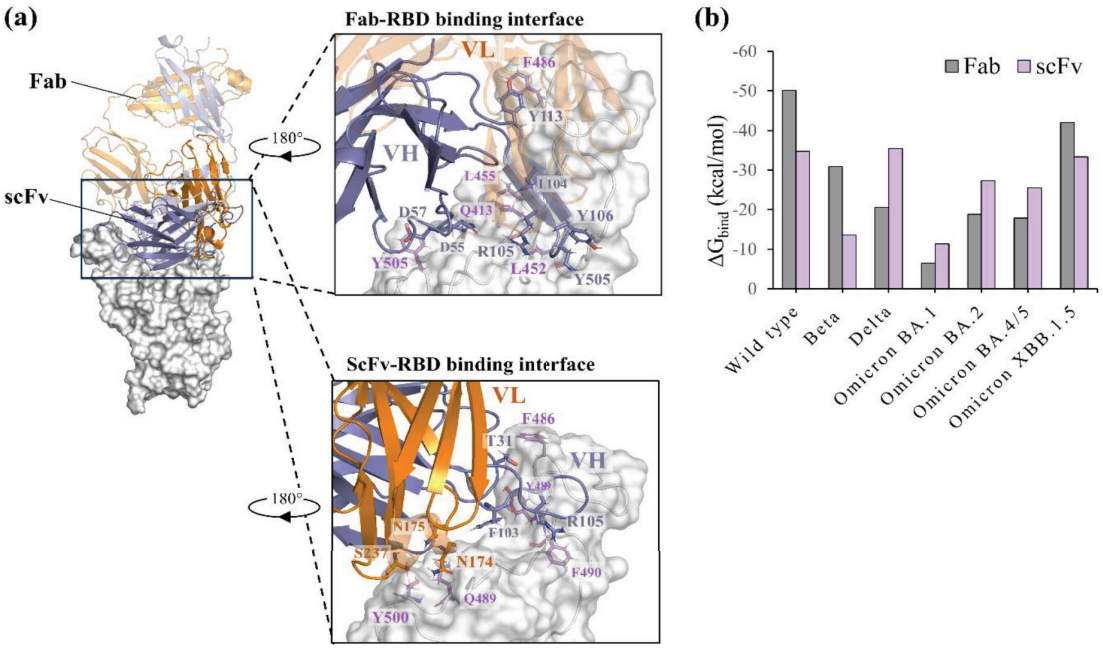

Figure 2 (a) The binding complex alignment and interaction residues on the binding interface of Fab-RBD (upper) and scFv-RBD (lower). Heavy or light chains are represented in light blue or orange, respectively. (b) Binding energy comparison of Fab and scFv binding each variant of RBD, which energy is calculated by MM/PBSA

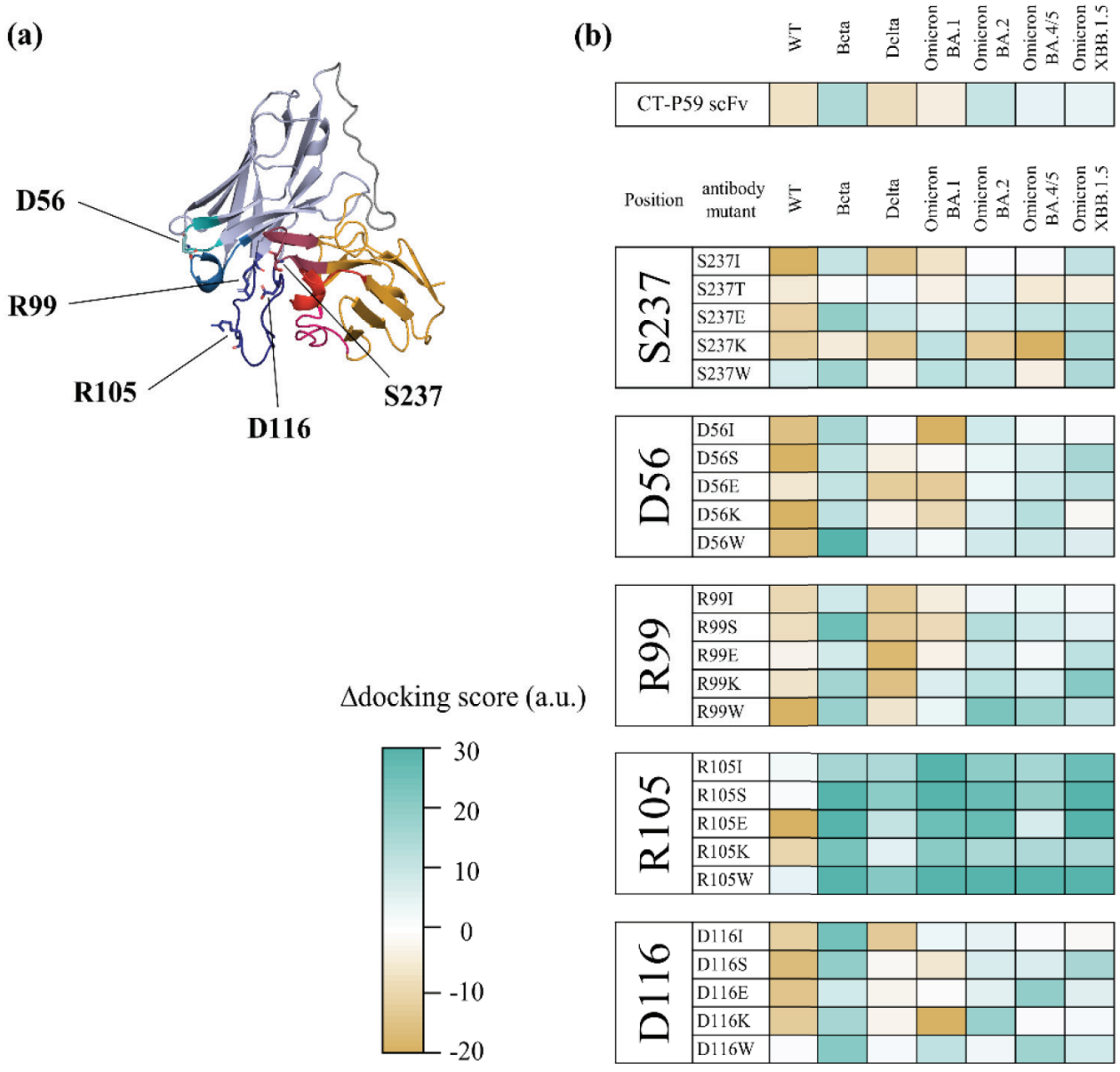

Figure 3 (a) Five mutated amino acids on scFv are marked. (b) A color map illustrates the relative difference between docking score of $scFv_{WT}$ and $scFv_{mutant}$ (Δdocking score = docking $score_{WT}$ – docking $score_{Mutant}$). The cyan color represents a positive Δdocking score (stronger binding) and the brown color represents a negative Δdocking score (weak binding). The results were calculated through HADDOCK 2.4

Based on the analysis of relative binding energies shown in Figure 2b and Supplementary Figure 2, D56 had a positive ΔG_{res} in most of the scFv-RBD complexes, indicating that the residue does not favor binding with the variants of RBD. In contrast, R99 did not play a significant role in scFv binding complexes. However, R99 could form a loop that improves virus binding. R105 exhibited the most negative binding energy in the scFv-RBD_{WT} interaction, contributing significantly to the main interaction of the complex. Its binding energy increased in other VOCs. D116 played a significant role in the interaction between the heavy and light chains of the scFv based on structure, although it lacked binding interaction with RBD due to its distance from the antigen binding site. Finally, S237, an interaction residue of the light chain for scFv binding to RBD_{WT} (Figure 2a), showed more positive binding energy in the Beta and Omicron BA.1 variant; this significant alteration might lead to the loss of light chain interaction (Supplementary Figure 2).

We conducted molecular docking of each singly mutated scFv to investigate the effects of mutant antibodies on VOCs and to enhance their neutralizing efficacy. It's important to note that each scFv protein underwent only a single mutation. The 25 mutant models were docked against RBD and screened based on their docking scores, as shown in Figure 3b. As compared to CT-P59 Fab, we found that most of the scFv variants exhibited more negative docking scores, indicating stronger interactions with Beta, Omicron BA.2, BA.4/5, and XBB.1.5. The Trp-mutated scFv binding to VOC RBDs emerged as the good variant, as indicated by more negative docking scores than other mutant scFvs.

The R105W variant provided the highest positive Δdocking score to the RBD of VOCs as compared to other R105 variants. Notably, R105 mutations in binding with the Delta variant also provided a more positive Δdocking score, whereas other mutations did not.

Broad neutralizing potential of CT-P59 scFv variant (R105W) against RBD of various VOC

The best-docked R105 variants showed that R105W is the most promising for confirming molecular docking results with MD simulation.

The $scFv_{R105W}$ provided better binding affinity by exhibiting more negative binding energy than that of CT-P59 Fab in Delta and Omicron variants (Figure 4a). The R105W mutation demonstrated the stability of scFv binding to VOC RBD, as indicated by a small distance change in overall conformation (smooth RMSD line) under physiological conditions (Figure 4b).

To assess the binding energy per residue in Supplementary Figure 3, the mutated W105 was identified as the main interaction residue with the lowest ΔG_{res} in every binding variant, except in the case of Delta and Omicron XBB.1.5, where W55 instead exhibited the lowest ΔG_{res}. After simulations, the binding modes of $scFv_{R105W}$ that interact with all RBD variants were different from those of $scFv_{WT.}$ At binding regions of all RBD variants, we found that $scFv_{R105W}$ used W105 as the common residue to bind all RBD variants. The W105 interacted with the residues Y452, F486, and Y489 on RBD (compare Figure 5a to 5b).

Discussion

Here, computational methods were employed to design, screen, and develop potential drugs for treating COVID-19 by analyzing the molecular interactions and binding affinities between the drug and the virus. We investigated the interaction between the antibody and the viral RBD to represent the initial step of inhibition and to identify candidate-neutralizing antibodies for COVID-19 and new variants.

The predicted structure of CT-P59 scFv binding RBD complex after performing MD simulations shows better neutralization efficiency as compared to Fab against the

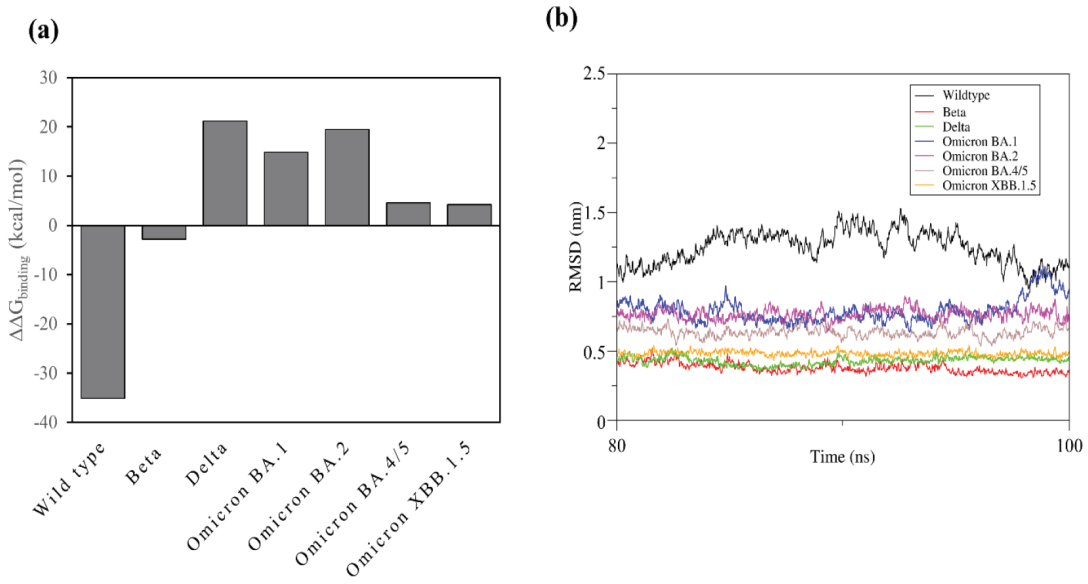

Figure 4 (a) Binding energy comparison ($\Delta\Delta G_{binding} = \Delta G_{WT} - \Delta G_{R105W}$) of Fab and $scFv_{R105W}$ binding to each variant of RBD. These energies were calculated using MM/PBSA, where a positive $\Delta\Delta G_{binding}$ indicates better affinity and a negative $\Delta\Delta G_{binding}$ indicates less affinity. (b) Root-mean-square deviation (RMSD) of each complex of $scFv_{R105W}$ binding a different RBD (WT and VOC) is shown as a different color in the last equilibrium 20 ns from 100 ns MD simulations

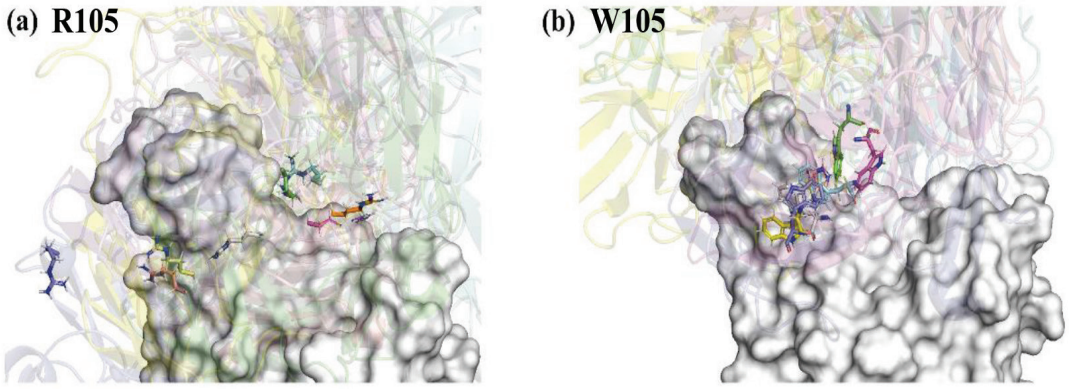

Figure 5 Alignment of binding modes for scFv antibody binding to various RBD variants. The RBDs are overlapped to visualize the binding positions of scFv. (a) Binding of $scFv_{WT}$ to RBD, highlighting the position of R105. (b) Binding of $scFv_{R105W}$ to RBD, highlighting the position of W105. The RBD is depicted in gray surface representation, while R105 and W105 are shown in licorice representation. Different scFvs are shown in transparent ribbons

Delta, BA.2, and BA.4/5 variants of the coronavirus. Even in the wild-type variant, the scFv utilizes both chains in the binding energy, but it is still weaker than Fab. However, both scFv and Fab use CDRH3 as the main interaction of the active site, with R105 as a key residue[4]. The mutation of Beta variant at N501Y, a site where scFv used the light chain to bind, resulted in a loss of binding site for this variant, which has the same binding effect as with Omicron BA.1. The Delta and Omicron XBB.1.5 complexes showed very low binding energies which are -35.48 and -33.33 kcal/mol respectively due to the use of all three heavy chain CDR loops (CDRH1-3) and the light chain, while BA.2 binds with the three heavy chain loops but is disrupted by D56, causing an increase in total binding energy. It was found that the binding efficiency of the scFv was suboptimal compared to the Fab fragment, indicating that the scFv might not be as effective in neutralizing the virus without further modifications. However, its high quantity of interaction residues indicated promise due to its greater flexibility compared to Fab[12]. The antibody might need significant modifications to enhance its binding efficiency. In this work, the $scFv_{WT}$ was thus modified at specific weak interaction points.

A molecular docking study was used to screen these mutant antibodies, particularly improving R105, and all Delta variants showed better binding with scFv. The strongest binding affinity was observed with the R105W mutation, which was further confirmed in MD simulations. The $scFv_{R105W}$ exhibited the highest binding affinity, demonstrating its potential for COVID-19 inhibition. Furthermore, $scFv_{R105W}$ displayed better binding affinity compared to CT-P59 against various variants and showed enhanced stability in binding complexes. The role of W105 was found to induce scFv binding to particular regions on the RBD, including Y452, F486, and Y489—a region that is conserved among coronaviruses[13]. Additionally, F486 was identified as a crucial position that promotes the binding of the XBB.1.5 variant to ACE2[5]. These findings underscore the importance of targeting this interaction blockade, which has led to the development of antibodies capable of broad neutralization.

In this study, we examined the binding of potential drug candidates and the whole virus using the binding interference interaction, represented by antibody fragments and RBD. The structural and interaction insights gained from this work are crucial for understanding and developing effective anti-COVID-19 drugs. However, these findings are preliminary and require further validation through in vitro and in vivo studies.

Conclusion

The computational design scFv aimed at neutralizing COVID-19 variants has identified $scFv_{R105W}$ as a promising candidate. Notably, our findings imply that $scFv_{R105W}$ also exhibited potential as a broad neutralizing drug and emphasized the importance of exploring scFv variants for their ability to combat the evolving new variants of COVID-19.

Acknowledgement

We would like to thank the Department of Biomedical Sciences and Biomedical Engineering, Faculty of Medicine, Prince of Songkla University for the research facility provided.

Funding sources

This research was supported by National Science, Research and Innovation Fund (NSRF) and Prince of Songkla University (Grant No. SCI6701067S), and partially supported by Development and Promotion of Science and Technology Talents Project (DPST).

Conflict of interest

There are no potential conflicts of interest to declare.

References

1. Lan J, Ge J, Yu J, Shan S, Zhou H, Fan S, et al. Structure of the SARS-CoV-2 spike receptor-binding domain bound to the ACE2 receptor. Nature 2020;581:215–20.
2. Laurini E, Marson D, Aulic S, Fermeglia A, Pricl S. Computational mutagenesis at the SARS-CoV-2 spike protein/angiotensin-converting enzyme 2 binding interface: comparison with experimental evidence. ACS Nano 2021;15:6929–48.
3. Jawad B, Adhikari P, Podgornik R, Ching WY. Impact of BA.1, BA.2, and BA.4/BA.5 Omicron mutations on therapeutic monoclonal antibodies. Comput Biol Med 2023;167.
4. Kim C, Ryu DK, Lee J, Kim Y Il, Seo JM, Kim YG, et al. A therapeutic neutralizing antibody targeting receptor binding domain of SARS-CoV-2 spike protein. Nat Commun 2021;12.
5. Andre M, Lau LS, Pokharel MD, Ramelow J, Owens F, Souchak J, et al. From alpha to omicron: how different variants of concern of the SARS-Coronavirus-2 impacted the world. Biology (Basel) 2023;12:1267.
6. Ebihara T, Masuda A, Takahashi D, Hino M, Mon H, Kakino K, et al. Production of scFv, Fab, and IgG of CR3022 antibodies against SARS-CoV-2 using silkworm-baculovirus expression system. Mol Biotechnol 2021;63:1223–34.
7. Van Zundert GCP, Rodrigues JPGLM, Trellet M, Schmitz C, Kastritis PL, Karaca E, et al. The HADDOCK2.2 web server: user-friendly integrative modeling of biomolecular complexes. J Mol Biol 2016;428:720–5.
8. Dominguez C, Boelens R, Bonvin AMJJ. HADDOCK: A protein-protein docking approach based on biochemical or biophysical information. J Am Chem Soc 2003;125:1731–7.
9. Janeway CA Jr, Travers P, Walport M, Shlomchik MJ. Immunobiology: the immune system in health and disease. 5th edition. New York: Garland Science; 2001.
10. Abraham MJ, Murtola T, Schulz R, Páll S, Smith JC, Hess B, et al. Gromacs: high performance molecular simulations through multi-level parallelism from laptops to supercomputers. SoftwareX 2015;1–2:19–25.
11. Huang J, Rauscher S, Nawrocki G, Ran T, Feig M, De Groot BL, et al. CHARMM36m: an improved force field for folded and intrinsically disordered proteins. Nat Methods 2017;14:71–3.
12. Bitencourt ALB, Campos RM, Cline EN, Klein WL, Sebollela A. Antibody fragments as tools for elucidating structure-toxicity relationships and for diagnostic/therapeutic targeting of neurotoxic amyloid oligomers. Int J Mol Sci 2020;21:1–18.
13. Olukitibi TA, Ao Z, Warner B, Unat R, Kobasa D, Yao X. Significance of Conserved Regions in Coronavirus Spike Protein for Developing a Novel Vaccine against SARS-CoV-2 Infection Vaccines (Basel) 2023;11:545.

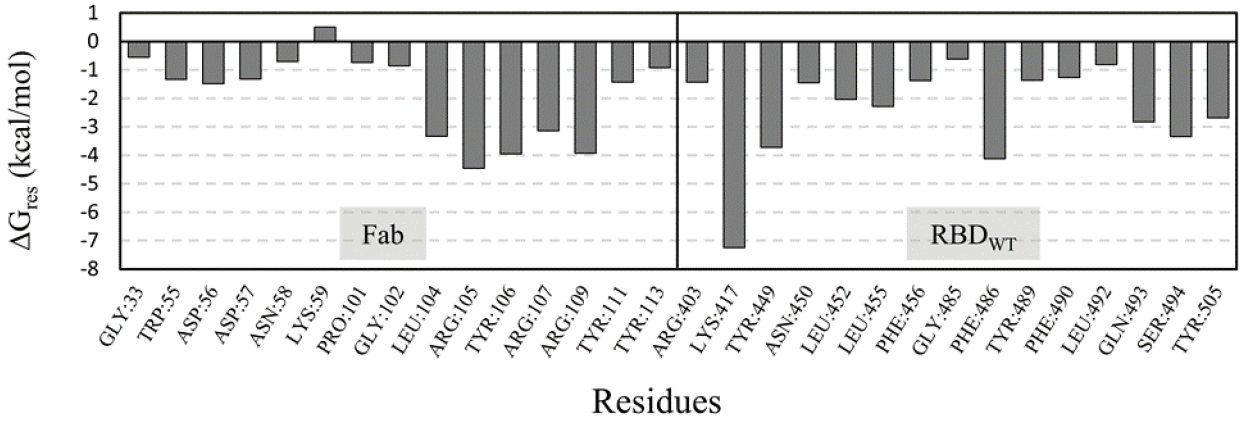

Supplementary Figure 1 The per-residue energy decomposition analysis of main residues of binding residues between Fab and RBD_{WT}

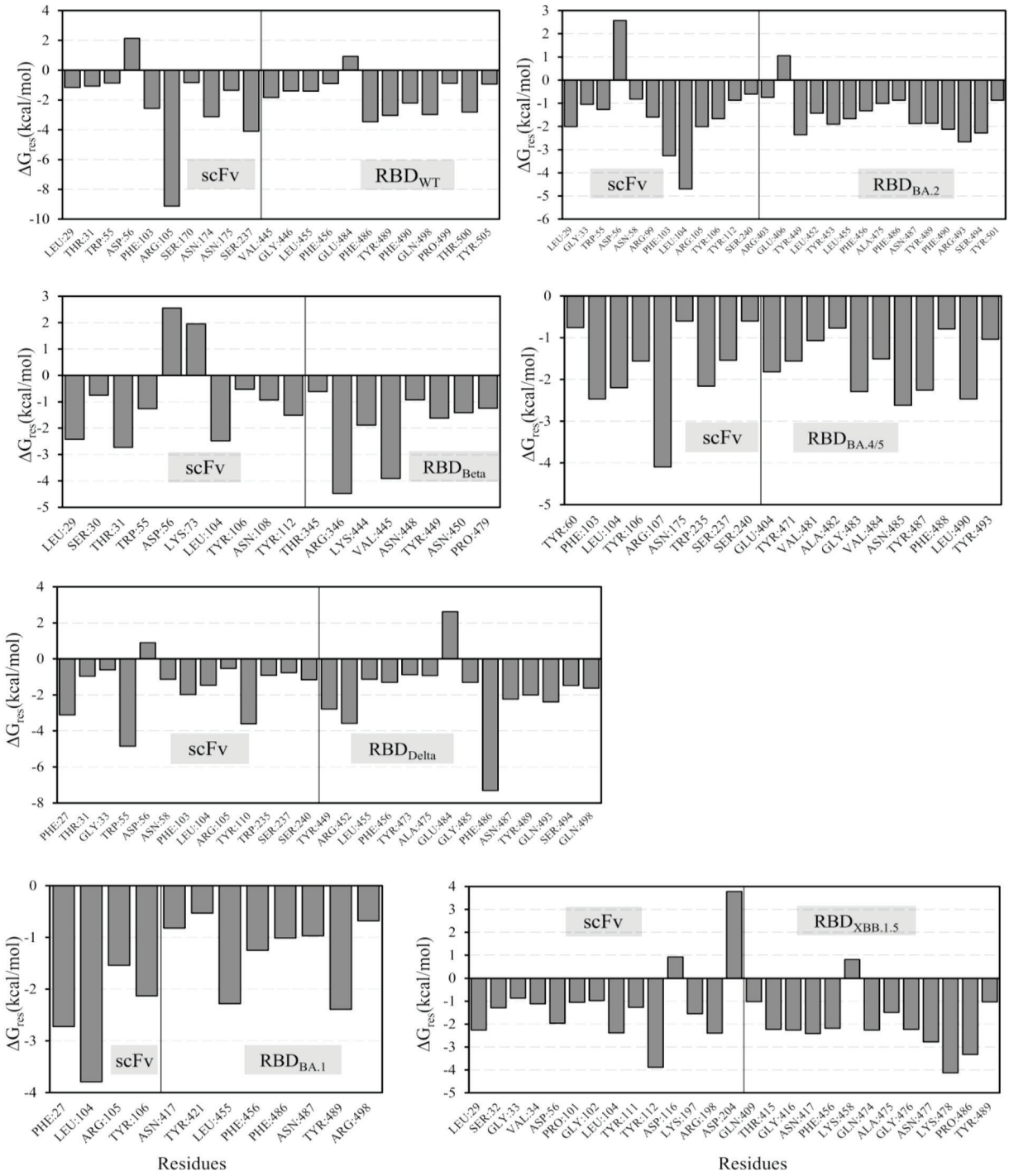

Supplementary Figure 2 Per-residue energy decomposition analysis of binding residues between scFv and each variant of the SARS-CoV-2 RBD. The binding complexes demonstrated include scFv-RBD_{WT}, scFv-RBD_{Beta}, scFv-RBD_{Delta}, scFv-$RBD_{BA.1}$, scFv-$RBD_{BA.2}$, scFv-$RBD_{BA.4/5}$, and scFv-$RBD_{XBB.1.5}$, respectively

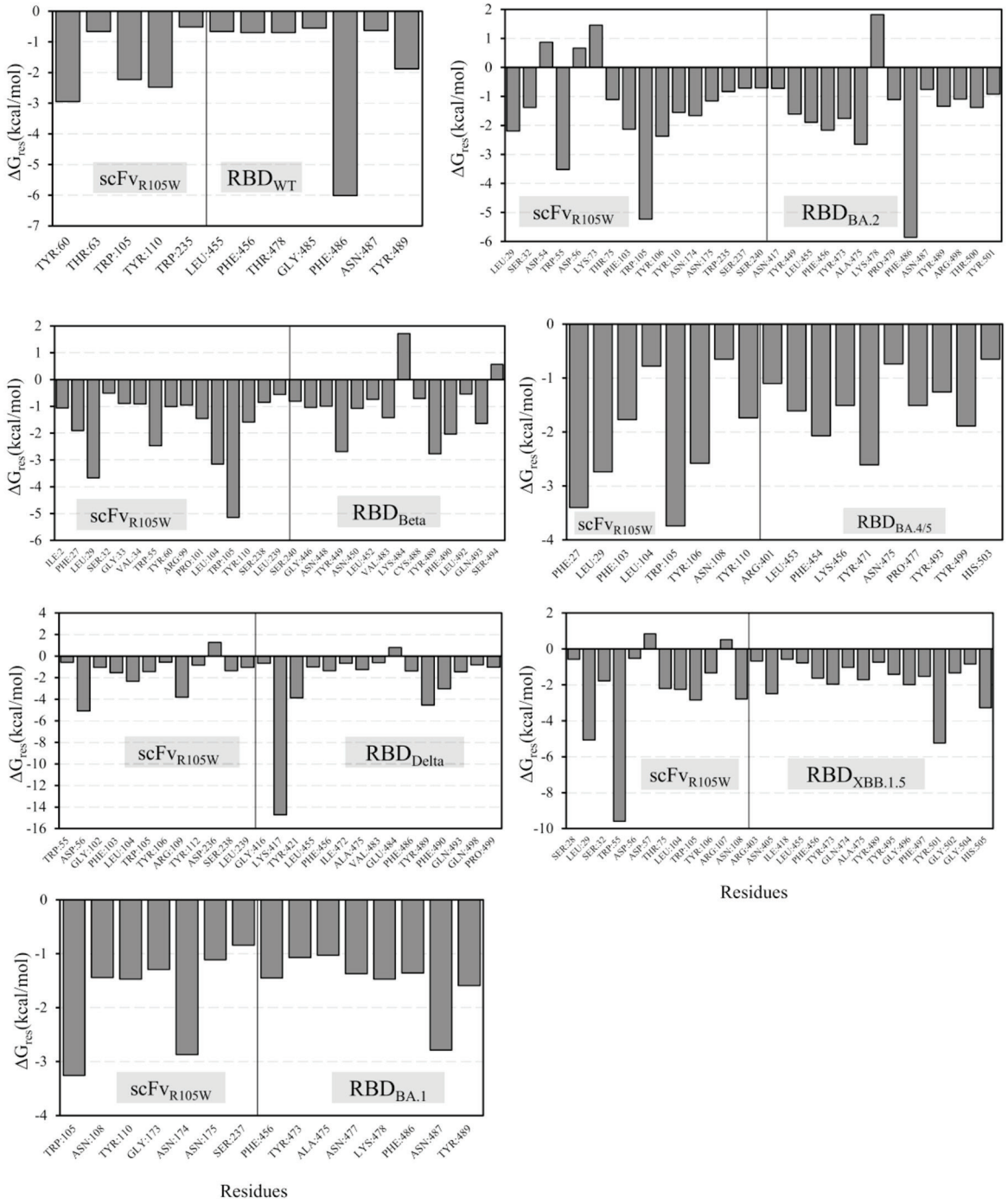

Supplementary Figure 3 Per-residue energy decomposition analysis of binding residues between $scFv_{R105W}$ and each variant of the SARS-CoV-2 RBD. The binding complexes demonstrated include $scFv_{R105W}$–RBD_{WT}, $scFv_{R105W}$–RBD_{Beta}, $scFv_{R105W}$–RBD_{Delta}, $scFv_{R105W}$–$RBD_{BA.1}$, $scFv_{R105W}$–$RBD_{BA.2}$, $scFv_{R105W}$–$RBD_{BA.4/5}$, and $scFv_{R105W}$–$RBD_{XBB.1.5}$, respectively